




Article

Preparation of Magnetic Nano-Catalyst Containing Schiff Base Unit and Its Application in the Chemical Fixation of CO₂ into Cyclic Carbonates

Na Kang ¹, Yindi Fan ^{1,2}, Dan Li ¹, Xiaoli Jia ¹ and Sanhu Zhao ^{1,2,*} ¹ Department of Chemistry, Xinzhou Normal University, Xinzhou 034000, China; jiaxiaoli@xztnu.edu.cn (X.J.)² School Chemistry and Material Science, Shanxi Normal University, Taiyuan 030000, China

* Correspondence: sanhuzhao@163.com or sanhuzhao@xztnu.edu.cn

Abstract: The development of a catalyst for the conversion of CO₂ and epoxides to the corresponding cyclic carbonates is still a very attractive topic. Magnetic nano-catalysts are widely used in various organic reactions due to their magnetic separation and recycling properties. Here, a magnetic nano-catalyst containing a Schiff base unit was designed, synthesized and used as a heterogeneous catalyst to catalyze CO₂ and epoxides to form cyclic carbonates without solvents and co-catalysts. The catalyst was characterized using Fourier transform infrared (FTIR), X-ray diffraction (XRD), thermogravimetric (TG), VSM, SEM, TEM and BET. The results show that the magnetic nano-catalyst containing the Schiff base unit has a high activity in the solvent-free cycloaddition reaction of CO₂ with epoxide under mild conditions, and is easily separated from the reaction mixture driven by external magnetic force. The recovered catalyst maintains a high performance after five cycles.

Keywords: magnetic nano-catalyst; Schiff base; carbon dioxide; cyclic carbonate



Citation: Kang, N.; Fan, Y.; Li, D.; Jia, X.; Zhao, S. Preparation of Magnetic Nano-Catalyst Containing Schiff Base Unit and Its Application in the Chemical Fixation of CO₂ into Cyclic Carbonates. *Magnetochimistry* **2024**, *10*, 33. <https://doi.org/10.3390/magnetochimistry10050033>

Academic Editor: Qianwang Chen

Received: 29 February 2024

Revised: 23 April 2024

Accepted: 23 April 2024

Published: 26 April 2024

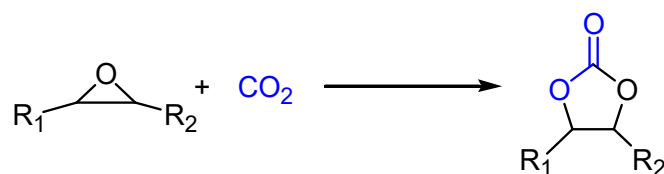


Copyright: © 2024 by the authors. Licensee MDPI, Basel, Switzerland. This article is an open access article distributed under the terms and conditions of the Creative Commons Attribution (CC BY) license (<https://creativecommons.org/licenses/by/4.0/>).

1. Introduction

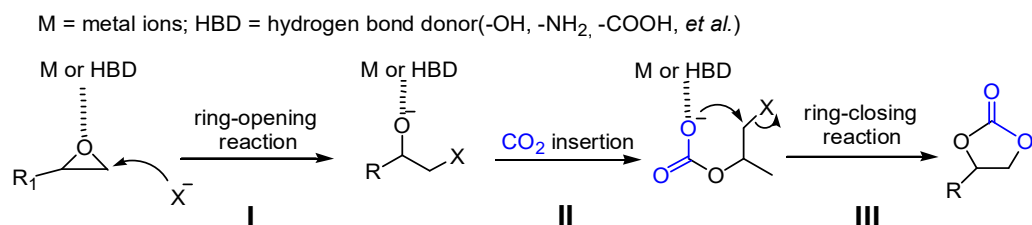
Carbon dioxide (CO₂) is the main greenhouse gas in the atmosphere, and is also an abundant, inexpensive, non-toxic, non-flammable renewable C₁ resource in nature. Using CO₂ as a cheap C₁ resource can not only replace toxic gases such as phosgene and carbon monoxide to produce high value-added products, but also alleviate environmental and climate problems, which has the effect of solving two problems at once. However, due to the unique delocalized electronic structure of CO₂, it has a high chemical stability and kinetic inertia in the catalytic conversion process, and often needs to use high temperature and high pressure and other harsh conditions [1]. Therefore, in the chemical reaction involving CO₂, it is necessary to introduce highly active reaction substrates and adopt catalytic technology to reduce the activation energy of the reaction [2]. At present, in the field of CO₂ utilization, two research directions have attracted much attention; one is the study of converting CO₂ into hydrocarbons such as methane, methanol and formic acid using photocatalysis and electrocatalysis technologies [3], and the other is the study of preparing cyclic carbonate or polycarbonate using the cycloaddition reaction of CO₂ with highly active small molecule epoxides [4]. For the coupling reaction of CO₂ with small molecule epoxides (Scheme 1), on the one hand, this reaction has atomic economy, can replace the traditional phosgene process, and meets the requirements of green chemistry and environmental protection [5]. On the other hand, the prepared cyclic carbonate is a very scarce chemical product with excellent physical and chemical properties, such as a high boiling point, high polarity, low volatility, good biodegradability and solubility, and is widely used in the fields of polar high boiling point aprotic solvent, lithium-ion battery electrolyte, pharmaceutical intermediates and polymer monomers [6]. At present, the homogeneous KI system is used in industry to

catalyze the synthesis of cyclic carbonates, but the production scale is small, the catalytic process requires harsh reaction conditions (180–200 °C, 5–8 MPa), and the separation of the catalyst and product is difficult [1].



Scheme 1. Reaction of epoxide with CO₂.

In view of the problems faced in the synthesis of cyclic carbonates from industrial fixed CO₂, the optimal solution is to start from the reaction mechanism and develop high efficiency catalysts. For the cycloaddition reaction between CO₂ and epoxide, the generally accepted reaction mechanism is a three-step reaction mechanism (Scheme 2): (I) activation and ring-opening of epoxides; (II) CO₂ insertion; (III) intramolecular nucleophilic substitution (closed-loop reaction).



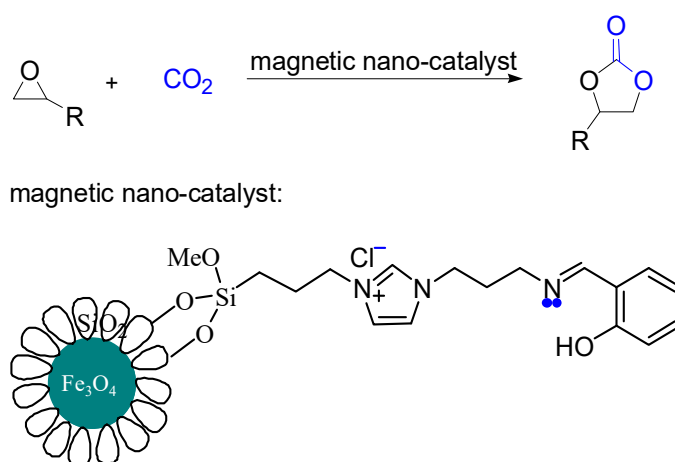
Scheme 2. Typical reaction mechanism for the cycloaddition of CO₂ to epoxide.

In the whole cycloaddition reaction, experimental and theoretical studies have shown that the activation and ring-opening of epoxides are the decisive step [7]. Catalysts for epoxide activation such as metal oxides [8], metal salts [9], metal complexes [10], metal-organic skeleton materials [11], rare earth complexes [12], supported organometallic complexes [13], COF [14], small molecules [15], porous carbon from biomass [16], plasma [17], and Rhodamine dyes [18] have been reported. Among them, metal ion modified catalysts account for a large proportion, and the metals involved are potassium, calcium, magnesium, aluminum, zinc, iron, copper, niobium, chromium, zirconium, cobalt, lanthanum, indium and so on. In the catalytic reaction process, metal ions mainly realize the activation of epoxide molecules by binding oxygen atoms in epoxide, and promote the cycloaddition reaction of epoxide. Other catalysts, such as pentaerythritol [19], cyclodextrin [20], lignin [21] and cellulose [22] can activate epoxides mainly through hydrogen bonding, which can effectively avoid the use of transition metals and meet the needs of green chemistry and sustainable development [23]. However, the relatively weak hydrogen bonding effect of metal-free catalysts has a weak promotion effect on the activation and ring-opening of epoxides, resulting in the harsh reaction conditions of high temperature, high pressure and high concentration of CO₂. Fixing CO₂ at a low temperature and normal pressure is still a challenge.

In terms of the design of the catalyst for the cycloaddition reaction of CO₂ and epoxide, the methods in the literature mainly focus on the activation of epoxide through hydrogen bond and cocatalyst (nucleophilic group X[−]). To a certain extent, the catalytic effect is obvious, but the overall catalytic effect is limited because the second step CO₂ insertion reaction is also a reaction with a high energy barrier. If the catalyst can activate the epoxide to promote its addition to CO₂, and can activate CO₂ at the same time, it will undoubtedly make the whole reaction easier. Based on the report about the activation of CO₂ via nitrogen-containing organic bases [24], we guessed that a multifunctional catalyst integrating hydrogen bond donor(HBD) group, N active center (Lewis base) and

nucleophilic ion (X^-) could reduce the reaction energy barrier to the maximum extent through the synergistic activation of CO_2 and epoxide, and should be an efficient catalyst for the cycloaddition reaction of CO_2 and epoxide.

Magnetic nano-catalysts, which have a high specific surface area and are able to have organic molecules loaded onto their surface, can provide more active sites [25], high catalytic activity, easy separation and recovery [26]. Based on our research on magnetic nano-catalysts [27] and functional ionic liquids [28,29], we designed and developed a magnetic nano-catalyst containing a Schiff base unit, which not only has HBD group, an N active center (the nitrogen atom in the Schiff base contains a lone pair of electrons, which can activate carbon dioxide molecules) and a nucleophilic ion (X^-), but also has the advantages of high catalytic activity, easy separation and recovery in the cycloaddition reaction of epoxide with CO_2 (Scheme 3).



Scheme 3. Cycloaddition reaction of epoxide with CO_2 catalyzed using the magnetic nano-catalyst containing Schiff base unit.

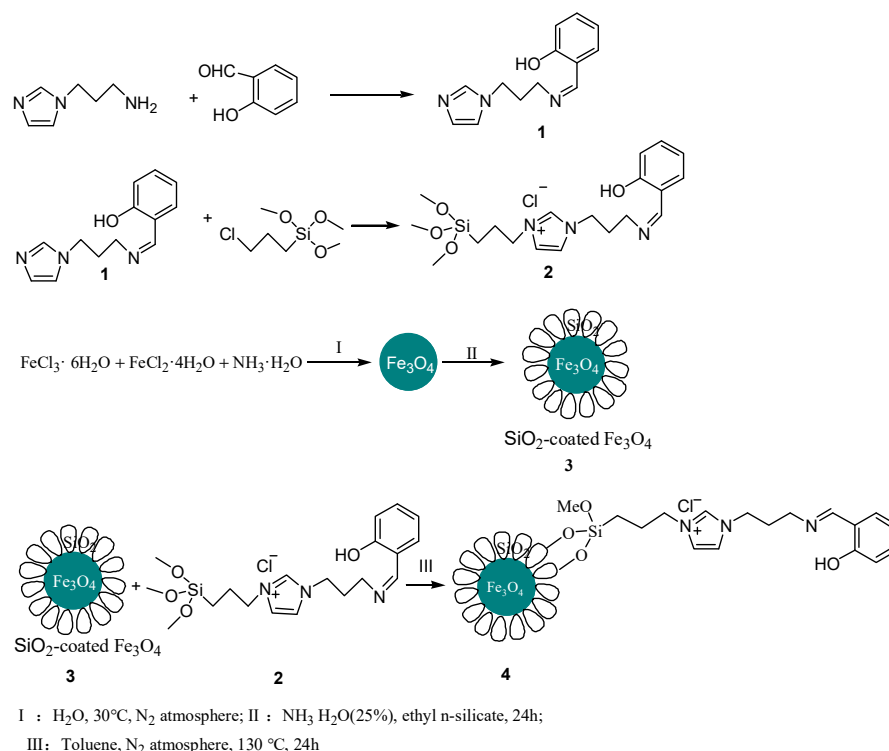
2. Materials and Methods

2.1. Materials

All chemical reagents were obtained from commercial suppliers and used without further purification.

2.2. Synthesis of 2-(3-(1H-Imidazol-1-yl)propyliminomethyl)phenol (Schiff Base 1)

This compound was prepared according to the literature procedure [30,31] with the following modifications: 6.25 g (0.05 mol) 1-(3-aminopropyl) imidazole was added to 50 mL anhydrous ethanol and then 6.10 g (0.05 mol) salicylaldehyde was added. Under the protection of a nitrogen atmosphere, the mixture was slowly heated to the reflux state with a magnetic stirrer and finally stabilized at 60 °C for 48 hours. Then, it was cooled to room temperature, the ethanol layer was removed, and the yellow solid Schiff base 1 containing imidazole ring (Scheme 4) was obtained using vacuum drying. M.p. 84–85 °C. Yield: 99.2%. 1H NMR (500 MHz, $DMSO-d_6$) δ 13.37 (s, 1H, OH), 8.54 (s, 1H, CH=), 7.64 (s, 1H, CH=), 7.45 (d, J = 9.3 Hz, 1H, CH=), 7.34 (t, J = 9.3 Hz, 1H, CH=), 7.21 (s, 1H, Ar-H), 6.89 (t, J = 7.1 Hz, 3H, Ar-H), 4.04 (t, J = 7.1 Hz, 2H, N-CH₂), 3.53 (t, J = 6.7 Hz, 2H, N-CH₂), 2.13–2.07 (m, 2H, CH₂); ^{13}C NMR (126 MHz, $DMSO-d_6$) δ 166.45, 160.53, 137.28, 132.35, 131.72, 128.54, 119.29, 118.67, 118.60, 116.44, 55.49, 43.85, 31.63.



Scheme 4. Synthetic routes of magnetic nano-catalyst containing Schiff base unit.

2.3. Synthesis of Ionic Liquid 2

A total of 2.29 g (10 mmol) Schiff base **1** (Scheme 4) containing an imidazole ring was added to a 50 mL round bottom flask containing 10 mL toluene, then 1.99 g (10 mmol) 3-chloropropyltrimethoxysilane was added under the protection of nitrogen. The reaction mixture was stirred at 110°C for 48 h and a yellowish viscous liquid 4.10 g (Yield: 95.8%) was obtained after removing the residual solvent toluene using rotary evaporation. ^1H NMR (500 MHz, $\text{DMSO}-d_6$) δ 13.11 (s, 1H, OH), 9.32 (s, 1H, CH=), 8.58–8.60 (m, 1H, CH=), 7.78–7.88 (m, 2H, CH=), 7.45 (d, $J = 7.2$ Hz, 1H, ArH), 7.34 (s, 1H, ArH), 6.90 (t, $J = 8.5$ Hz, 2H, ArH), 4.28–4.31 (m, 2H, NCH_2), 4.06–4.17 (m, 2H, NCH_2), 3.65 (t, $J = 6.5$ Hz, 2H, NCH_2), 3.36–3.47 (m, 9H, OCH_3), 3.17 (d, $J = 3.8$ Hz, 2H, CH_2), 2.20–2.26 (m, 2H, CH_2), 1.79–1.86 (m, 2H, SiCH_2); ^{13}C NMR (126 MHz, $\text{DMSO}-d_6$) δ 165.93, 159.72, 135.63, 131.80, 131.71, 130.02, 121.87, 118.04, 118.00, 115.78, 54.85, 49.51, 47.96, 30.89, 29.68, 22.58, 4.80.

2.4. Synthesis of Magnetic Nanoparticles Fe_3O_4

Magnetic Fe_3O_4 particles were prepared using the co-precipitation method [32]. $\text{FeCl}_3 \cdot 6\text{H}_2\text{O}$ (8.1 g, 30 mmol) and $\text{FeCl}_2 \cdot 4\text{H}_2\text{O}$ (3.4 g, 17 mmol) were added to a 250 mL round-bottom flask containing 100 mL distilled water. Under the protection of nitrogen, the reaction mixture was first stirred at room temperature for 30 min. When all components were dissolved, 35 mL (25%) of $\text{NH}_3 \cdot \text{H}_2\text{O}$ was added quickly, then stirred for 30 min at 30°C under nitrogen protection. The solid product was collected and washed with deionized water until the solution remained neutral. Then, it was repeatedly washed with anhydrous ethanol for 2–3 times, and the residual solvent was removed using a vacuum method to obtain black crystalline particles of Fe_3O_4 .

2.5. Synthesis of Magnetic Nanoparticles $\text{Fe}_3\text{O}_4 @ \text{SiO}_2$

A layer of silica was coated on the surface of Fe_3O_4 using the sol-gel method [33,34]. With the assistance of ultrasound, 2.0 g (8.64 mmol) of Fe_3O_4 magnetic nanoparticles was dispersed into 150 mL anhydrous ethanol and 30 mL deionized water; after stirring the reaction mixture for 30 min, 4 mL concentrated ammonia and 13 mL ethyl orthosilicate were added and stirred at room temperature for 24 h under nitrogen protection. The magnetic

solid was collected using magnetic force, washed with deionized water to neutral, then washed with anhydrous ethanol 2–3 times; a gray-brown solid powder 3.9 g was obtained after the residual ethanol was removed using rotary evaporation.

2.6. Synthesis of Magnetic Nano-Catalyst Containing Schiff Base Unit

Then, 4 g (9.33 mmol) ionic liquid 2 was dispersed in 10 mL toluene and then 4 g $\text{Fe}_3\text{O}_4@\text{SiO}_2$ was added. The reaction was refluxed at 110 °C for 24 h under the protection of nitrogen. The resulting magnetic nanoparticles were collected using an external magnet, washed with anhydrous ethanol for 2–3 times, and dried using rotary evaporation to obtain a brown solid powder 7.1 g.

2.7. General Method of Cycloaddition of Epoxides with CO_2

The epoxy compound (0.04475 mol) and the catalyst were added to a 50 mL autoclave which was connected to a high-pressure carbon dioxide gas cylinder, and the CO_2 was transported at a constant pressure during the catalytic process. The reaction mixture was gently stirred at a set temperature and time. After the reaction was completed, the reaction was cooled to room temperature and the crude product was obtained after the magnetic transfer of the catalyst. For the products 4-methyl-[1,3]dioxolan-2-one, 4-chloromethyl-[1,3]dioxolan-2-one and 4-butyl-1,3-dioxolan-2-one, almost pure products were obtained. For the products 4-phenyl-[1,3]dioxolan-2-one and hexahydro-benzo[1,3]dioxol-2-one, the crude products were purified using column chromatography (hexane: ethyl acetate = 3:1) to afford the desired cyclic carbonate. All products were characterized using NMR spectroscopy and the data are listed as follows.

4-Methyl-[1,3]dioxolan-2-one

Light yellow liquid; ^1H NMR (500 MHz, CDCl_3) δ 4.82–4.90 (m, 1H, OCH), 4.56 (q, J = 7.7, 8.4 Hz, 1H, OCH_2), 4.03 (q, J = 7.2, 8.4 Hz, 1H, OCH_2), 1.48 (d, J = 6.3 Hz, 3H, CH_3); ^{13}C NMR (126 MHz, CDCl_3) δ 155.13, 73.59, 70.69, 19.54.

4-Chloromethyl-[1,3]dioxolan-2-one

Light yellow liquid; ^1H NMR (500 MHz, CDCl_3) δ 4.94–4.99 (m, 1H, OCH), 4.56–4.62 (q, J = 8.2, 8.9 Hz, 1H, OCH_2), 4.40–4.44 (q, J = 5.7, 8.9 Hz, 1H, OCH_2), 3.76–3.80 (q, J = 5.8, 12.0 Hz, 1H, CH_2Cl), 3.69–3.75 (q, J = 3.7, 12.0 Hz, 1H, CH_2Cl); ^{13}C NMR (126 MHz, CDCl_3) δ 155.38, 74.82, 67.99, 44.12.

4-Phenyl-[1,3]dioxolan-2-one

Light yellow liquid; ^1H NMR (500 MHz, CDCl_3) δ 7.42–7.47 (m, 3H, C_6H_5), 7.35–7.38 (q, J = 2.1, 7.6 Hz, 2H, C_6H_5), 5.68 (t, J = 8.0 Hz, 1H, OCH), 4.81 (t, J = 8.4 Hz, 1H, OCH_2), 4.35 (t, J = 8.3 Hz, 1H, OCH_2); ^{13}C NMR (126 MHz, CDCl_3) δ 154.93, 135.73, 129.74, 129.21, 125.86, 78.07, 71.15.

Hexahydro-benzo[1,3]dioxol-2-one

Light yellow liquid; ^1H NMR (500 MHz, CDCl_3) δ 4.65–4.71 (m, 2H, OCH), 1.85 (t, J = 7.6 Hz, 4H, CH_2), 1.57 (t, J = 7.6 Hz, 2H, CH_2), 1.38–1.43 (m, 2H, CH_2); ^{13}C NMR (126 MHz, CDCl_3) δ 155.67, 75.87, 26.86, 19.28.

4-Butyl-1,3-dioxolan-2-one

Light yellow liquid; ^1H NMR (500 MHz, CDCl_3) δ 4.72–4.67 (m, 1H, OCH_2), 4.62–4.57 (m, 1H, OCH_2), 4.20–4.11 (m, 1H, OCH), 1.82–1.60 (m, 2H, CH_2), 1.52–1.20 (m, 4H, CH_2CH_2), 0.92 (t, J = 7.0 Hz, 3H, CH_3). ^{13}C NMR (126 MHz, CDCl_3) δ 155.2, 77.2, 69.5, 33.7, 26.5, 22.4, 13.9.

2.8. Characterization Techniques

X-ray diffraction (XRD) images were obtained by using an XRD-6100 device with $\text{Cu K}\alpha$ radiation (λ = 0.15418 nm). Infrared spectroscopy (FTIR) was obtained using an IR

Affinit-IS Fourier Transform Spectrometer. A thermogravimetric analysis image (TG) was obtained from a thermogravimetric analyzer STA 449F5 operating at 220 V and 16 A in the atmosphere of nitrogen. Scanning electron microscope (SEM) images were performed on a FESEM FEI Quanta 400 FEG (FEI Quanta, Waltham, MA, USA). The vibrating sample magnetometer (VSM) mode was performed using SQUID-VSM (America Quantum Design, San Diego, CA, USA). Brunner–Emmet–Teller (BET) analysis was recorded using the automated specific surface area and porosity analyzer TriStar II 3020 (America Micromeritics, Columbia, America). ^1H NMR (500 MHz) and ^{13}C NMR (126 MHz) were recorded on a 500 MHz spectrometer (Bruker AVANCE NEO 500M, Karlsruhe, Germany) with $\text{DMSO-}d_6$ or CDCl_3 as solvent.

3. Results and Discussion

As shown in Scheme 4, the Schiff base **1** containing an imidazole ring was synthesized using 1-(3-aminopropyl) imidazole with salicylic aldehyde, and the ionic liquid **2** containing the Schiff base structure was synthesized using the reaction of 3-chloropropyltrimethoxysilane with Schiff base **1**. Then, under nitrogen protection, the ionic liquid **2** was selected to condense with $\text{Fe}_3\text{O}_4@\text{SiO}_2$ in toluene and the final magnetic nano-catalyst containing the Schiff base unit **4** was achieved. For the nano Fe_3O_4 and $\text{Fe}_3\text{O}_4@\text{SiO}_2$, they were prepared using the method reported in the reference [25].

3.1. XRD Analysis

The composition and structure of magnetic nanoparticles Fe_3O_4 , $\text{Fe}_3\text{O}_4@\text{SiO}_2$ and the magnetic nano-catalyst containing the Schiff base unit were confirmed using X-ray diffraction (XRD). As shown in Figure 1, peaks at 30.0° , 35.4° , 43.0° , 53.4° , 56.9° , and 62.5° , consistent with the peak of standard Fe_3O_4 and the plate peaks at $18\text{--}28^\circ$, indicate the formation of amorphous silicon shells around Fe_3O_4 .

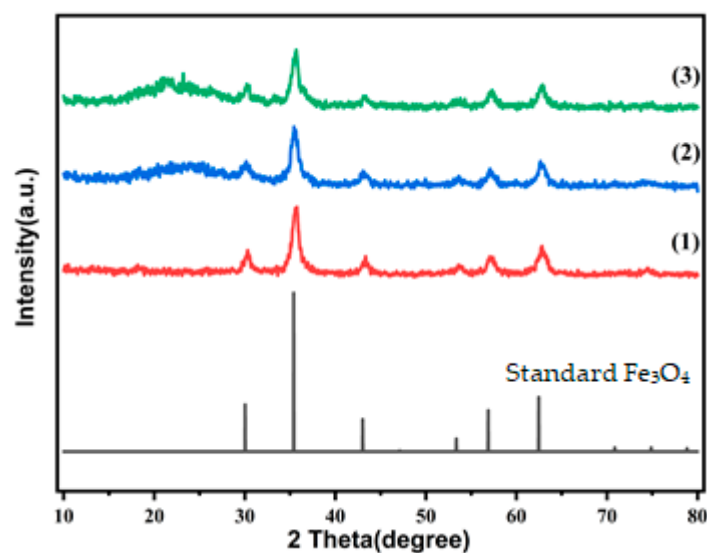


Figure 1. XRD patterns of nanoparticles. (1) Fe_3O_4 , (2) $\text{Fe}_3\text{O}_4@\text{SiO}_2$, (3) magnetic nano-catalyst containing Schiff base unit.

3.2. FTIR Analysis

To further determine the functional group and the structure of the magnetic nanoparticles, FTIR spectroscopy was also performed. As shown in Figure 2, the peak at 608 cm^{-1} is the characteristic peak of the Fe–O bond stretching vibration, and the broad peak at 1074 cm^{-1} is the characteristic peak of the Si–O bond stretching vibration. The characteristic peaks at 2992 cm^{-1} and 3022 cm^{-1} in curve (3) are related to the C–H bond stretching vibration, indicating that the alkyl load is on the magnetic nanoparticles. The peak at 1672 cm^{-1} in curve (3) is the characteristic peak of the C=N bond stretching, the peak at

1626, 1454 cm^{-1} is the characteristic peak of the benzene ring skeleton vibration, and the peak at 3415 cm^{-1} is the characteristic peak of O–H bond stretching, which means that the Schiff base unit is attached to the magnetic nanoparticles $\text{Fe}_3\text{O}_4/\text{SiO}_2$.

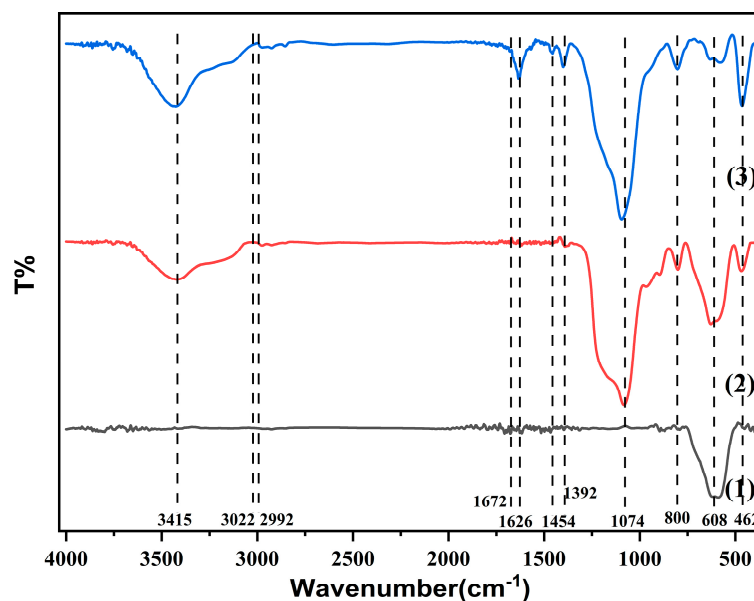


Figure 2. FTIR spectra of nanoparticles. (1) Fe_3O_4 , (2) $\text{Fe}_3\text{O}_4/\text{SiO}_2$, (3) magnetic nano-catalyst containing Schiff base unit.

3.3. TG Analysis

In order to investigate the structure, composition and thermal stability of magnetic nanoparticles, we carried out TG analysis in the temperature range of 25–1000 °C. The curve (1) is the mass loss diagram of magnetic nano- Fe_3O_4 , which, as can be seen from Figure 3, magnetic nano- Fe_3O_4 has two obvious mass loss stages; the first stage is from 25 °C to 200 °C, with a mass loss of 1.15%, which may be due to the evaporation of physically adsorbed water or residual solvents. The second stage is 200–700 °C and the mass loss is 2.87%, which may be caused by the decomposition of the hydroxyl group on the surface of Fe_3O_4 . Coupled with a minimum loss of 0.11% above 700 °C, the final mass loss is 4.13%. The curve (2) is the mass loss diagram of magnetic nano- $\text{Fe}_3\text{O}_4/\text{SiO}_2$. It can be seen that the magnetic nano- $\text{Fe}_3\text{O}_4/\text{SiO}_2$ has two obvious mass loss stages. The first stage is from 25 to 150 °C and the mass loss is 5.83%, which may be due to the evaporation of water or the physical adsorption of residual solvent. In the second stage, from 150 to 700 °C, the mass loss is 4.56%, which may be due to the decomposition of the silicon shell. Coupled with a minimum loss of 0.65% above 700 °C, the final mass loss is 11.04%. The curve (3) is the mass loss diagram of the magnetic nano-catalyst containing the Schiff base unit. It can be seen that there are three obvious stages of quality loss. The first stage is from 25 to 230 °C and the mass loss is 1.77%, which may be due to the evaporation of water or the physical adsorption of residual solvents. The second stage is from 230 to 320 °C and the mass loss is 4.29%, which may be caused by the surface cracking of the Schiff base unit. In the third stage, from 320 to 820 °C, the mass loss is 14.15%, which may be due to the decomposition of the silicon shell, and the final mass loss is 20.21%. Comparing the TG analysis data of $\text{Fe}_3\text{O}_4/\text{SiO}_2$ and magnetic nano-catalyst containing the Schiff base unit, about 9.17% of the Schiff base ionic liquid is loaded onto the magnetic nano-catalyst containing the Schiff base unit. The active sites of the 1 g magnetic nano-catalyst is equivalent to about 0.11 mmol of the Schiff base ionic liquid 2. Through the TG analysis and comparison of the mass loss curves of the magnetic nanoparticles, we can determine that each step of the preparation of the magnetic nano-catalyst is successful.

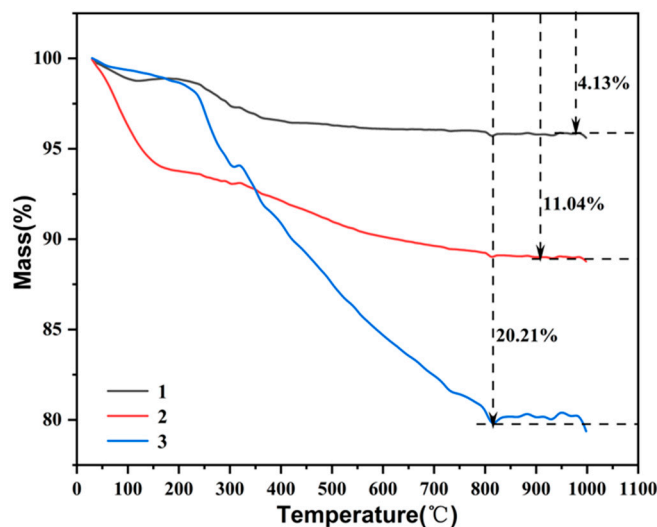


Figure 3. TG curves of nanoparticles. (1) Fe_3O_4 , (2) $\text{Fe}_3\text{O}_4@\text{SiO}_2$, (3) magnetic nano-catalyst containing Schiff base unit.

3.4. VSM Analysis

The magnetic measurement was carried out at room temperature and under the conditions of the applied magnetic field. VSM was used to scan the magnetic field from $-25,000$ to $25,000$ Oe, and the magnetic properties of the catalyst were measured. As shown in Figure 4, the catalyst has good paramagnetism and good dispersion in water. The catalyst dispersed in water can be quickly aggregated using external magnetic force, which proves that the catalyst can be applied and recovered in water reaction.

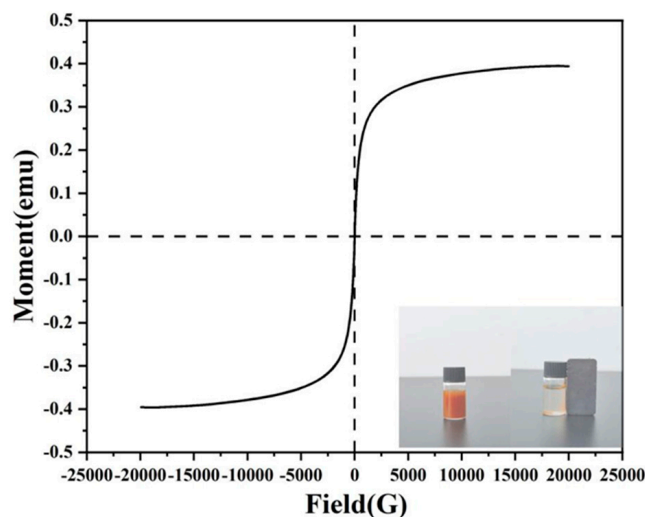


Figure 4. VSM image of magnetic nano-catalyst containing Schiff base unit.

3.5. SEM and TEM Analysis

As shown in Figure 5, the observation using scanning electron microscopy (SEM) reveals that the morphology of the core-shell magnetic nano-catalyst has a uniform size of $50\sim 150$ nm and the shape of the catalyst particles was approximately spherical. The agglomeration effect was also generated due to its magnetic effect, which makes the magnetic nano-catalyst easy to separate. Transmission electron microscopy (TEM) showed that Fe_3O_4 was coated with SiO_2 and ionic liquid, which was consistent with XRD and FTIR analysis.

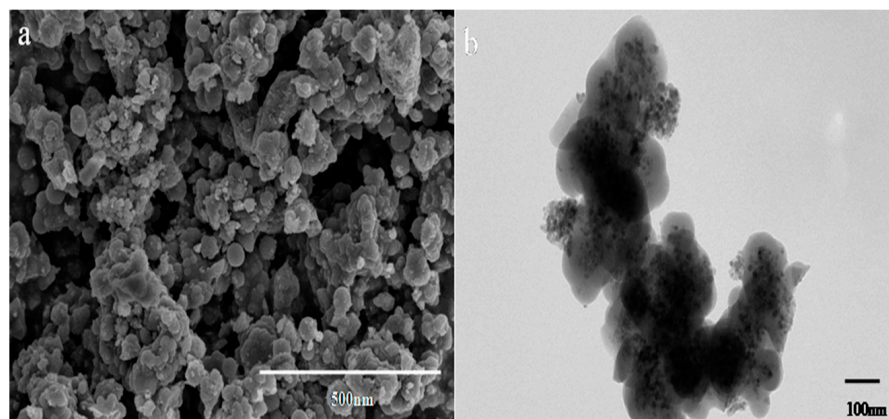


Figure 5. SEM (a) and TEM (b) images of magnetic nano-catalyst containing Schiff base unit.

3.6. BET Analysis

The adsorption–desorption isotherms of N_2 are shown in Figure 6. The hysteresis loop indicates that the catalyst belongs to mesoporous material. The surface area, pore volume and pore size of the magnetic nano-catalyst containing the Schiff base unit were determined using the BET test, and the BET data are as shown in Table 1. According to the pore size and surface area of the catalyst, combined with the catalytic effect experiment, the nano-catalyst can effectively catalyze the cycloaddition reaction of epoxide and CO_2 to prepare the cyclic carbonate. The reason may be the combined effects of ion microenvironment, nano size, hydrogen bond effect and weak alkali environment.

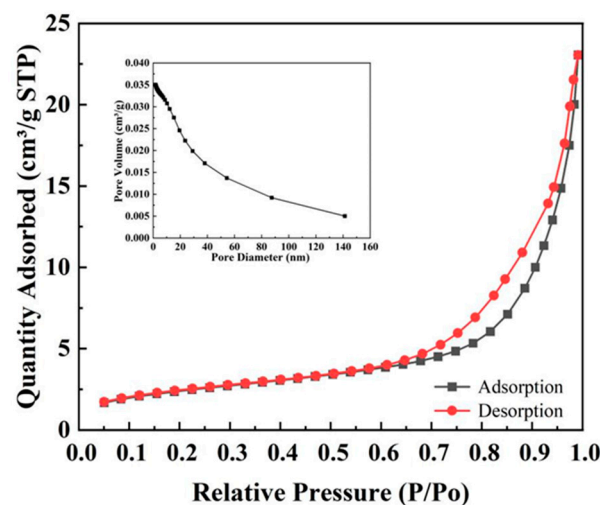


Figure 6. N_2 adsorption–desorption and pore size distribution curve.

Table 1. The results of BET surface area analysis.

Parameters		Magnetic Nano-Catalyst Containing Schiff Base Unit
Surface Area	Single point surface area at $P/P_o = 0.294306215$	$8.3206 \text{ m}^2/\text{g}$
	BET Surface Area	$8.6415 \text{ m}^2/\text{g}$
	Langmuir Surface Area	$13.0942 \text{ m}^2/\text{g}$
	t-Plot External Surface Area	$8.7656 \text{ m}^2/\text{g}$

Table 1. Cont.

Parameters		Magnetic Nano-Catalyst Containing Schiff Base Unit
Pore Volume	Single point adsorption total pore volume of pores less than 181.2138 nm diameter at $P/P_0 = 0.989213975$	0.034517 cm ³ /g
	BJH Adsorption cumulative volume of pores between 1.7000 nm and 300.0000 nm diameter	0.035029 cm ³ /g
	BJH Desorption cumulative volume of pores between 1.7000 nm and 300.0000 nm diameter	0.035171 cm ³ /g
Pore Size	Adsorption average pore diameter (4V/A using BET)	15.97728 nm
	BJH Adsorption average pore diameter (4V/A)	16.7619 nm
	BJH Desorption average pore diameter (4V/A)	15.1738 nm

3.7. Effects of Reaction Parameters on the Catalytic Activity of Magnetic Nano-Catalyst Containing Schiff Base Unit

In order to test whether the magnetic nano-catalyst containing the Schiff base unit has catalytic activity, the reaction of epichlorohydrin with CO₂ was used as the model reaction to study the effect of various parameters on the reaction. First of all, we set the pressure of CO₂ to 3 atm, the reaction temperature to 120 °C, the amount of catalyst to 1.25 g and the reaction time to 15 h; we were delighted to find that almost all of the epichlorohydrin was converted into the target product, and a 99% yield of cyclic carbonate was obtained (Table 2, entry 1). Then, we tried to reduce the amount of catalyst, the pressure of the CO₂ and the reaction time (Table 2, entries 2–6); we found that when the catalyst dosage is 0.75 g, the pressure of CO₂ is 1 atm, and the reaction temperature is 120 °C, the yield of 99% can be obtained after 10 h (Table 2, entry 6). In order to find more optimal reaction conditions, the reaction temperature, time and catalyst dosage were further explored (Table 2, entries 7–10). The results showed that the corresponding cyclic carbonate was obtained with 99% yield when 0.75 g magnetic nano-catalyst was used in the reaction of epichlorohydrin (0.04475 mol) with CO₂ (1 atm) after 8 h at 100 °C.

Table 2. Exploration of reaction conditions ¹.

Entry	Magnetic Nano-Catalyst (g)	CO ₂ (atm)	Time (h)	Temperature (°C)	Yield ² (%)
1	1.25	3	15	120	99
2	1.25	2	15	120	99
3	1.00	2	15	120	99
4	1.00	2	10	120	99
5	0.75	2	10	120	99
6	0.75	1	10	120	99
7	0.75	1	10	100	99
8	0.50	1	10	100	94
9	0.75	1	8	100	99
10	0.75	1	6	100	93
11 ³	0.75	1	8	100	0
12 ⁴	0.75	1	8	100	82

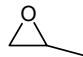
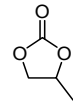
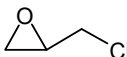
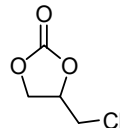
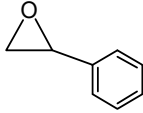
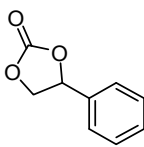
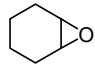
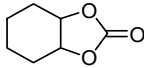
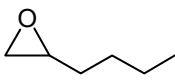
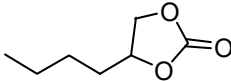
¹ General reaction conditions: epichlorohydrin (0.04475 mol); ² isolated yield; ³ using magnetic nanoparticle Fe₃O₄@SiO₂ as catalyst; ⁴ using 1-butyl-3-methylimidazole chloride as catalyst.

In order to further explore the catalytic sites, magnetic nanoparticle Fe₃O₄@SiO₂ and 1-butyl-3-methylimidazole chloride were used, respectively, in the model reaction as catalysts. For the magnetic nanoparticle Fe₃O₄@SiO₂, no product was detected, and for the imidazole ionic liquid, when 0.75 g (4 mmol) of catalyst was used, only 82% yield was achieved. According to TG analysis, the active sites of 0.75 g magnetic nano-catalyst is equivalent to about 0.08 mmol Schiff base ionic liquid 2, the content of the imidazolium ring is significantly lower than that of 1-butyl-3-methylimidazole chloride, but the yield

of the target product reaches 99%. This indicates that the key catalytic site of the magnetic nano-catalyst is not the hydrogen bonding of hydrogen at the C2 position of the imidazole ring, and the catalytic sites of the catalyst may be attributed to the hydrogen bonding of phenolic hydroxyl group and the alkalinity of Schiff bases.

To further test the generality of the catalyst, the magnetic nano-catalyst containing Schiff base unit has been used in the reaction of a series of epoxides fixing CO₂ to synthesize cyclic carbonates (Table 3). Both propylene oxide and epichlorohydrin yield the target products with 99% yields. For the 1,2-epoxyhexane, 82% yield was achieved. But for the sterically hindered 1-phenyl epoxide and 7-oxa-bicyclo[4.1.0]heptane, the target product is obtained at only 40% and 5% yields, respectively. It can be concluded that the reaction is favorable at the less hindered side of epoxide.

Table 3. Cycloaddition of CO₂ to various epoxides catalyzed using the magnetic nano-catalyst.

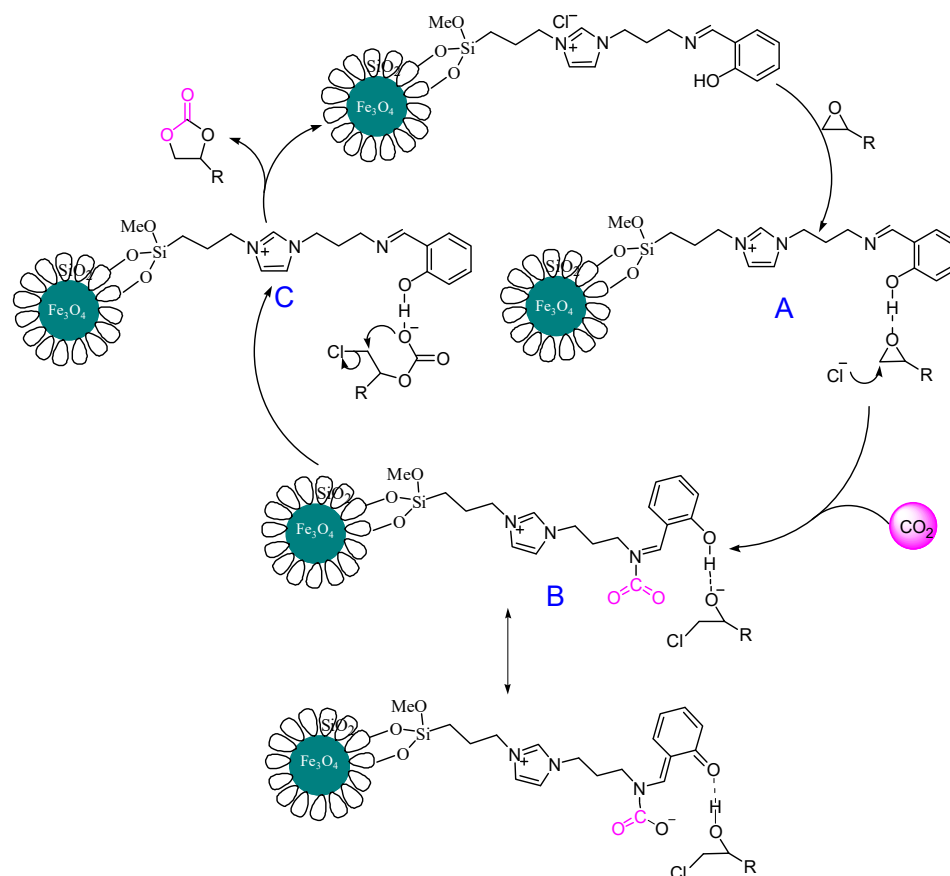
Entry ¹	Substrate	Product	Yield (%) ²
1			99
2			99
3			40
4			5
5			82

¹ General reaction conditions: catalyst (0.75 g), epoxide (0.04475 mol), CO₂ (99.999%, 1 atm), 100 °C, 8 h. ² Isolated yield.

3.8. Proposed Mechanism

The first use of imidazolium ILs as catalysts for the epoxide/CO₂ coupling was pioneered by Deng et al. [35]. The hydrogen bond between the proton in position 2 of the imidazolium ring with the O-donor group of epoxide plays an important role and the acidity of the C2 proton is crucial for the activation of the epoxide. For the present magnetic nano-catalyst containing the Schiff base unit, although there are imidazole rings, when comparing with the hydrogen bond between the hydrogen atom of phenol hydroxyl group and the O-donor group of epoxide, the hydrogen bond between the proton in position 2 of the imidazolium ring with the O-donor group of epoxide is obviously weaker. This can be seen from the ¹H NMR data of the Schiff base ionic liquid: the hydrogen chemical shift of phenol hydroxyl group is 13.11, and the chemical shift of the C2 proton is 9.32. To further investigate the activation of epoxides via hydrogen bonds, the ¹H NMR spectra of a mixture of Schiff base ionic liquid and epichlorohydrin was detected; a clear up field shift in the Schiff base ionic liquid OH proton signal was observed (from δ = 13.11 to 12.96 ppm), which indicates that the epoxide forms a hydrogen bond with the OH group. In addition, the lone pair electrons on nitrogen atoms in the Schiff base -N=C- can activate CO₂, which facilitates the coupling of carbon dioxide and epoxides. Therefore, the activation of a magnetic nano-catalyst was ascribed to the synergetic effects between CO₂ activation/capture through the -N=CH-C=C group of the Schiff base and hydrogen bond formation between the -OH group of phenol with the epoxide. Based on the previous research [22,24] and the results of

this experiment, the possible catalytic mechanism of magnetic nano-catalyst is proposed as shown in Scheme 5. The epoxy ring is activated through hydrogen bonding between the OH group on the benzene ring and the O atom of the epoxide. Simultaneously, the Cl^- anion nucleophilic ally attacks the less sterically hindered carbon atom of the epoxide ring to form the corresponding alcoholate. CO_2 is activated through the N atom of Schiff base, and the nucleophilic addition of the alcoholate to CO_2 forms an alkyl carbonate anion (C); the ring-closing of intermediate C affords the corresponding cyclic carbonate and regenerates the catalyst, thus the catalytic cycle was completed.



Scheme 5. The proposed mechanism for the coupling reaction of epoxide with CO_2 catalyzed using magnetic nano-catalyst containing Schiff base unit.

3.9. Recycling Research

In order to test the reusability of the magnetic nano-catalyst containing the Schiff base unit, the cycloaddition reaction of epichlorohydrin with CO_2 was carried out in the presence of a catalytic amount of magnetic nano-catalyst under optimal conditions. When the reaction is complete, the catalyst can be separated under the magnetic force for the next cycle. As shown in Table 4, the catalyst was cycled five times, and the yield hardly changed, which indicates that the structure of the catalyst is relatively stable.

Table 4. Reusability of the magnetic nano-catalyst containing Schiff base unit ^a.

Run	Time (h)	Isolated Yield/%
1	8	99
2	8	99
3	8	98
4	8	98
5	8	97

^a General reaction conditions: catalyst (0.75 g), epichlorohydrin (0.04475 mol), CO_2 (99.999%, 1 atm), 100 °C.

4. Conclusions

In summary, a functional magnetic nano-catalyst containing a Schiff base unit was prepared and applied as the catalyst for the chemical fixation of CO₂ into cyclic carbonates. The results show that the magnetic nano-catalyst has a high catalytic activity, making it a potential candidate catalyst for the synthesis of cyclic carbonates from CO₂ and epoxides under mild conditions. Notably, the magnetic nano-catalyst containing the Schiff base unit can be recycled for at least five times without any significant loss of activity, making this catalyst sustainable and economical. In addition, the catalyst has the advantages of good stability, magnetic recovery and relatively simple synthesis process, which is especially suitable for CO₂ conversion and green industrial chemical processes.

Supplementary Materials: The following supporting information can be downloaded at: <https://www.mdpi.com/article/10.3390/magnetochemistry10050033/s1>, Figure S1: NMR spectrum of 1-butyl-3-methylimidazolium chloride; Figure S2: NMR spectrum of the Schiff base containing imidazole ring; Figure S3: NMR spectrum of the ionic liquid containing Schiff base unit; Figure S4: NMR spectrum of a mixture of ionic liquid containing Schiff base unit and epichlorohydrin; Figure S5: NMR spectrum of 4-methyl-[1,3]dioxolan-2-one; Figure S6: NMR spectrum of 4-butyl-[1,3]dioxolan-2-one; Figure S7: NMR spectrum of 4-chloromethyl-[1,3]dioxolan-2-one; Figure S8: NMR spectrum of hexahydro-benzo[1,3]dioxol-2-one; Figure S9: NMR spectrum of 4-phenyl-[1,3]dioxolan-2-one.

Author Contributions: N.K. and Y.F. contributed equally to this work and are co-first authors. Writing—original draft preparation, N.K. and Y.F.; writing—review and editing, D.L. and X.J.; project administration, S.Z. All authors have read and agreed to the published version of the manuscript.

Funding: This research received financial support from National college student's innovation and entrepreneurship training program (No. 20230935) and Basic Research Project of Xinzhou Science and Technology Bureau (No. 20230509).

Institutional Review Board Statement: Not applicable.

Informed Consent Statement: Not applicable.

Data Availability Statement: The original contributions presented in the study are included in the article/Supplementary Materials, further inquiries can be directed to the corresponding author.

Conflicts of Interest: The authors declare no conflicts of interest.

References

1. Sakakura, T.; Choi, J.C.; Yasuda, H. Transformation of Carbon Dioxide. *Chem. Rev.* **2007**, *107*, 2365–2387. [\[CrossRef\]](#) [\[PubMed\]](#)
2. Alves, M.; Grignard, B.; Méreau, R.; Jerome, C.; Tassaing, T.; Detrembleur, C. OrganoCatalyzed Coupling of Carbon Dioxide with Epoxides for the Synthesis of Cyclic Carbonates: Catalyst Design and Mechanistic studies. *Catal. Sci. Technol.* **2017**, *7*, 2651–2684. [\[CrossRef\]](#)
3. Kattel, S.; Ramírez, P.J.; Chen, J.G.; Rodriguez, J.A.; Liu, P. Active Sites for CO₂ Hydrogenation to Methanol on Cu/ZnO Catalysts. *Science* **2017**, *355*, 1296–1299. [\[CrossRef\]](#) [\[PubMed\]](#)
4. Saini, S.; Khan, S.R.; Gour, N.K.; Deka, R.C.; Jain, S.L. Metal-free, Redox-neutral, and Visible Light-triggered Coupling of CO₂ with Epoxides to Cyclic Carbonates at Atmospheric Pressure. *Green Chem.* **2022**, *24*, 3644–3650. [\[CrossRef\]](#)
5. Claver, C.; Yeamin, M.B.; Reguero, M.; Masdeu-Bultó, A.M. Recent Advances in the Use of Catalysts Based on Natural Products for the Conversion of CO₂ into Cyclic Carbonates. *Green Chem.* **2020**, *22*, 7665–7706. [\[CrossRef\]](#)
6. Yu, W.; Maynard, E.; Chiaradia, V.; Arno, M.C.; Dove, A.P. Aliphatic Polycarbonates from Cyclic Carbonate Monomers and their Application as Biomaterials. *Chem. Rev.* **2021**, *121*, 10865–10907. [\[CrossRef\]](#)
7. Sun, H.; Zhang, D. Density Functional Theory Study on the Cycloaddition of Carbon Dioxide with Propylene Oxide Catalyzed by Alkylmethylimidazolium Chlorine Ionic Liquids. *J. Phys. Chem. A* **2007**, *111*, 8036–8043. [\[CrossRef\]](#)
8. Yamaguchi, K.; Ebitani, K.; Yoshida, T.; Yoshida, H.; Kaneda, K. Mg–Al Mixed Oxides as Highly Active Acid–base Catalysts for Cycloaddition of Carbon Dioxide to Epoxides. *J. Am. Chem. Soc.* **1999**, *121*, 4526–4527. [\[CrossRef\]](#)
9. Baalbaki, H.A.; Roshandel, H.; Hein, J.E.; Mehrkhodavandi, P. Conversion of Dilute CO₂ to Cyclic Carbonates at Sub-atmospheric Pressures by a Simple Indium Catalyst. *Catal. Sci. Technol.* **2021**, *11*, 2119–2129. [\[CrossRef\]](#)
10. Deacy, A.C.; Phanopoulos, A.; Lindeboom, W.; Buchard, A.; Williams, C.K. Insights into the Mechanism of Carbon Dioxide and Propylene Oxide Ring-opening Copolymerization Using a Co(III)/K(I) Heterodinuclear Catalyst. *J. Am. Chem. Soc.* **2022**, *144*, 17929–17938. [\[CrossRef\]](#)

11. Gu, Y.; Anjali, B.A.; Yoon, S.; Choe, Y.; Chung, Y.G.; Park, D.-W. Defect-engineered MOF-801 for Cycloaddition of CO₂ with Epoxides. *J. Mater. Chem. A* **2022**, *10*, 10051–10061. [[CrossRef](#)]
12. Qing, Y.; Liu, T.; Zhao, B.; Bao, X.; Yuan, D.; Yao, Y. Cycloaddition of Di-substituted Epoxides and CO₂ under Ambient Conditions Catalysed by Rare-earth Poly(phenolate) Complexes. *Inorg. Chem. Front.* **2022**, *9*, 2969–2979. [[CrossRef](#)]
13. Al Maksoud, W.; Saidi, A.; Samantaray, M.K.; Abou-Hamad, E.; Poater, A.; Ould-Chikh, S.; Guo, X.; Guan, E.; Ma, T.; Gates, B.C.; et al. Docking of Tetra-methyl Zirconium to the Surface of Silica: A Well-defined Pre-catalyst for Conversion of CO₂ to Cyclic Carbonates. *Chem. Commun.* **2020**, *56*, 3528–3531. [[CrossRef](#)]
14. Sani, R.; Dey, T.K.; Sarkar, M.; Basu, P.; Islam, S.M. A Study of Contemporary Progress Relating to COF Materials for CO₂ Capture and Fixation Reactions. *Mater. Adv.* **2022**, *3*, 5575–5597. [[CrossRef](#)]
15. Song, Q.W.; Ma, R.; Liu, P.; Zhang, K.; He, L.N. Recent Progress in CO₂ Conversion into Organic Chemicals by Molecular Catalysis. *Green Chem.* **2023**, *25*, 6538–6560. [[CrossRef](#)]
16. He, J.; Jin, Z.; Gan, F.; Xie, L.; Guo, J.; Zhang, S.; Jia, C.Q.; Ma, D.; Dai, Z.; Jiang, X. Liquefiable Biomass-derived Porous Carbons and their Applications in CO₂ Capture and Conversion. *Green Chem.* **2022**, *24*, 3376–3415. [[CrossRef](#)]
17. Guselnikova, O.; Postnikov, P.; Kosina, J.; Kolska, Z.; Trelin, A.; Svorcik, V.; Lyutakov, O. A Breath of Fresh Air for Atmospheric CO₂ Utilisation: A Plas Mon-assisted Preparation of Cyclic Carbonate at Ambient Conditions. *J. Mater. Chem. A* **2021**, *9*, 8462–8469. [[CrossRef](#)]
18. Chen, J.; Chiarioni, G.; Euverink, G.-J.W.; Pescarmona, P.P. Dyes as Efficient and Reusable Organocatalysts for the Synthesis of Cyclic Carbonates from Epoxides and CO₂. *Green Chem.* **2023**, *25*, 9744–9759. [[CrossRef](#)]
19. Wilhelm, M.E.; Anthofer, M.H.; Cokoja, M.; Markovits, I.I.E.; Herrmann, W.A.; Kühn, F.E. Cycloaddition of Carbon Dioxide and Epoxides Using Pentaerythritol and Halides as Dual Catalyst System. *Chem. Sus. Chem.* **2014**, *7*, 1357–1360. [[CrossRef](#)]
20. Song, J.; Zhang, Z.; Han, B.; Hu, S.; Li, W.; Xie, Y. Synthesis of Cyclic Carbonates from Epoxides and CO₂ Catalyzed by Potassium Halide in the Presence of β -cyclodextrin. *Green Chem.* **2008**, *10*, 1337–1341. [[CrossRef](#)]
21. Wu, Z.; Xie, H.; Yu, X.; Liu, E. Lignin-based Green Catalyst for the Chemical Fixation of Carbon Dioxide with Epoxides to form Cyclic Carbonates under Solvent-free Conditions. *Chem. Cat. Chem.* **2013**, *5*, 1328–1333. [[CrossRef](#)]
22. Sun, J.; Cheng, W.; Yang, Z.; Wang, J.; Xu, T.; Xin, J.; Zhang, S. Super base/Cellulose: An Environmentally Benign Catalyst for Chemical Fixation of Carbon Dioxide into Cyclic Carbonates. *Green Chem.* **2014**, *16*, 3071–3078. [[CrossRef](#)]
23. Guo, L.; Lamb, K.J.; North, M. Recent Developments in Organocatalysed Transformations of Epoxides and Carbon Dioxide into Cyclic Carbonates. *Green Chem.* **2021**, *23*, 77–118. [[CrossRef](#)]
24. Wang, L.; Zhang, G.; Kodama, K.; Hirose, T. An Efficient Metal- and Solvent-free Organocatalytic System for Chemical Fixation of CO₂ into Cyclic Carbonates under Mild Conditions. *Green Chem.* **2016**, *18*, 1229–1233. [[CrossRef](#)]
25. Zhang, X.; He, X.; Zhao, S. Preparation of a Novel Fe₃O₄@SiO₂@propyl@DBU Magnetic Core-shell Nanocatalyst for Knoevenagel Reaction in Aqueous Medium. *Green Chem. Lett. Rev.* **2021**, *14*, 85–98. [[CrossRef](#)]
26. Ndolomingo, M.J.; Bingwa, N.; Meijboom, R. Review of Supported Metal Nanoparticles: Synthesis Methodologies, Advantages and Application as Catalysts. *J. Mater. Sci.* **2020**, *55*, 6195–6241. [[CrossRef](#)]
27. Jia, X.; Zhang, X.; Wang, Z.; Zhao, S. Tertiary Amine Ionic Liquid Incorporated Fe₃O₄ Nanoparticles as a Versatile Catalyst for the Knoevenagel Reaction. *Synthetic Commun.* **2022**, *52*, 774–786. [[CrossRef](#)]
28. Meng, D.; Qiao, Y.; Wang, X.; Wen, W.; Zhao, S. DABCO-catalyzed Knoevenagel Condensation of Aldehydes with Ethyl Cyanoacetate Using Hydroxyl Ionic Liquid as a Promoter. *RSC Adv.* **2018**, *8*, 30180–30185. [[CrossRef](#)]
29. Zhao, S.; Meng, D.; Wei, L.; Qiao, Y.; Xi, F. Novel DBU-based Hydroxyl Ionic Liquid for Efficient Knoevenagel Reaction in Water. *Green Chem. Lett. Rev.* **2019**, *12*, 271–277. [[CrossRef](#)]
30. McGinley, J.; McCann, M.; Ni, K.; Tallon, T.; Kavanagh, K.; Devereux, M.; Ma, X.; McKee, V. Imidazole Schiff Base Ligands: Synthesis, Coordination Complexes and Biological Activities. *Polyhedron* **2013**, *55*, 169–178. [[CrossRef](#)]
31. Qian, H.; Dai, Y.; Geng, J.; Wang, L.; Wang, C.; Huang, W. A Flexible Multidentate Schiff-base Ligand Having Multifarious Coordination modes in Its Copper(II) and Cadmium(II) Complexes. *Polyhedron* **2014**, *67*, 314–320. [[CrossRef](#)]
32. Bu, D.L.; Li, N.; Zhou, Y.; Feng, H.Y.; Yu, F.; Cheng, C.X.; Li, M.; Xiao, L.H.; Ao, Y.H. Enhanced UV Stability of N-Halamine-Immobilized Fe₃O₄@SiO₂@TiO₂ Nanoparticles: Synthesis, Characteristics and Antibacterial Property. *New J. Chem.* **2020**, *44*, 10352–10358. [[CrossRef](#)]
33. Choi, H.J.; Piao, S.H.; Kim, S.D.; Chae, H.S. Core-shell Structured Fe₃O₄@SiO₂ Nanoparticles Fabricated by Sol-gel Method and their Magnetorheology. *Colloid Polym. Sci.* **2016**, *294*, 647–655. [[CrossRef](#)]
34. Chen, X.; Du, S.; Hong, R.; Chen, H. Preparation of RGO/Fe₃O₄ Nanocomposites as a Microwave Absorbing Material. *Inorganics* **2023**, *11*, 143. [[CrossRef](#)]
35. Peng, J.; Deng, Y. Cycloaddition of Carbon Dioxide to Propylene Oxide Catalyzed by Ionic Liquids. *New J. Chem.* **2001**, *25*, 639–641. [[CrossRef](#)]

Disclaimer/Publisher's Note: The statements, opinions and data contained in all publications are solely those of the individual author(s) and contributor(s) and not of MDPI and/or the editor(s). MDPI and/or the editor(s) disclaim responsibility for any injury to people or property resulting from any ideas, methods, instructions or products referred to in the content.